

## Modelling Liquefied Natural Gas Vaporization Rate for Water Spills

Ezeh E.A<sup>1\*</sup> and Okafor E.J<sup>1</sup>

<sup>1</sup>Department of Petroleum and Gas Engineering, University of Port Harcourt, Nigeria.

\*Corresponding author's email: [amandianaezee@yahoo.com](mailto:amandianaezee@yahoo.com)

### Abstract

Natural gas is preferred energy source because of its high energy content and minimal environmental impact when contrasted with other fossil fuels. When transporting natural gas from production to consumption locations, especially over long distances, natural gas is typically converted to liquid form for ease and cost-effectiveness. Generation and behaviour of hazardous liquefied natural gas (LNG) vapour is greatly determined by vaporization rate of LNG. For the purpose of risk assessment and consequence analysis of possible LNG spill, it is crucial to estimate vaporization rate of LNG spill on confined water surface, since LNG spill often result in explosion and fire which can lead to large scale accidents. An approach to prediction of LNG vaporization rate is proposed. Within the framework of model derived herein, influence of LNG pool height on vaporization rate of LNG pool, modelled as pure methane on confined water surface, has been investigated. The model's solution was implemented in FORTRAN environment, an integrated development environment for an instantaneous LNG spill scenario. Overall simulation results indicated that vaporization rate of LNG pool on confined water surface depends on LNG pool height, temperature of water surface and heat flux amongst other factors.

**Keywords:** Liquefied natural gas, LNG vaporization rate, LNG spills

Received: 15<sup>th</sup> September, 2023

Accepted: 2<sup>nd</sup> December, 2023

### 1. Introduction

In recent years, demand for natural gas has been on the increase. This can be attributed to high caloric value of natural gas, economic incentives, and the fact that natural gas is clean burning fossil fuel. Stranded natural gas can be conveniently transported from producing nations to consuming nations via water, when liquefied. Ships carrying Liquefied natural gas (LNG) are usually double-hulled, and carry up to sixty thousand tonnes of LNG. Liquefied natural gas (LNG) may be stored in storage tank situated in diked area, which could be water-logged.

Liquefaction process of natural gas allows a 600-fold decrease in the volume of the gas being transported (Michelle et al., 2012). The resulting liquid which is mainly composed of methane

presents some hazardous properties linked to its inflammable nature and its cryogenic state. Upon release on water, LNG will boil vigorously and generate vapour that will disperse or form white dense vapour cloud. If the LNG vapour concentration is within flammability range of 5% - 15%, the vapour may ignite when there is source of ignition and cause fires, explosions occur under certain defined conditions.

It is very pertinent to explain clearly some features of LNG spill on water surface, as a result of accidental LNG release which may happen across the LNG value chain such as when LNG storage tank is punctured, or during loading or unloading of liquefied natural gas (LNG). Fig. 1 is a schematic diagram of processes which may concurrently occur upon spillage of LNG on water surface.

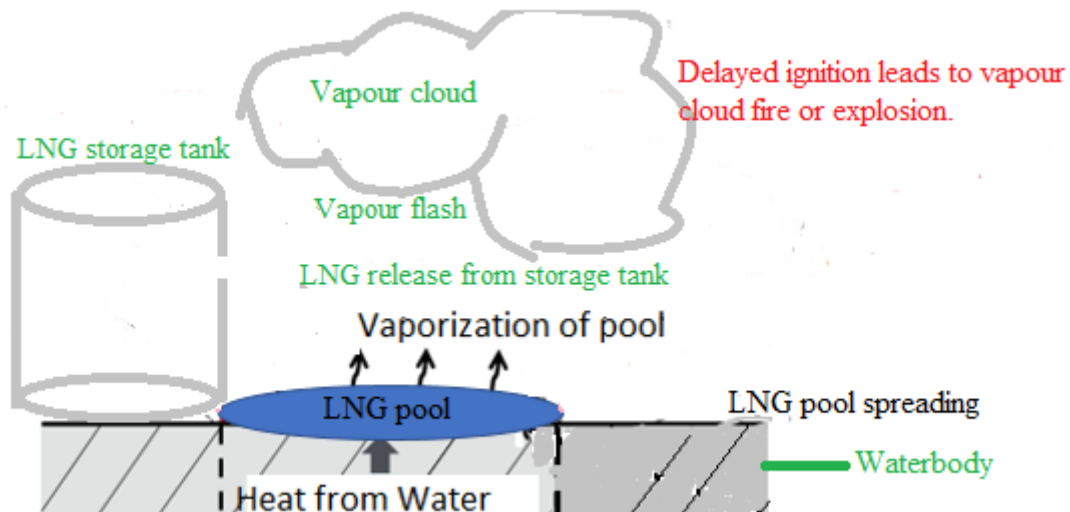


Fig. 1: LNG spill configuration.

In Fig. 1, LNG spills through orifice on LNG storage tank. Some parts of the LNG jet spontaneously produce vapour termed vapour flash, due to flash vaporization. Whereas integral part of the LNG jet is spills on water surface, the water surface serves as heat source for vaporization of LNG pool forming on it. LNG density is approximately  $423 \text{ kg/m}^3$  while density of water is about  $1000 \text{ kg/m}^3$ . This implies that LNG is less

dense than water, thus, LNG forms a buoying pool on water surface. Spreading of LNG pool on water surface portrays divergence from a centre. The LNG pool spreads out radially, and boils in three consecutive regimes, namely, film boiling regime, transition boiling regime and nucleate boiling regime as shown in Fig. 2. Heat flux from underlying water into LNG pool influences LNG boiling.

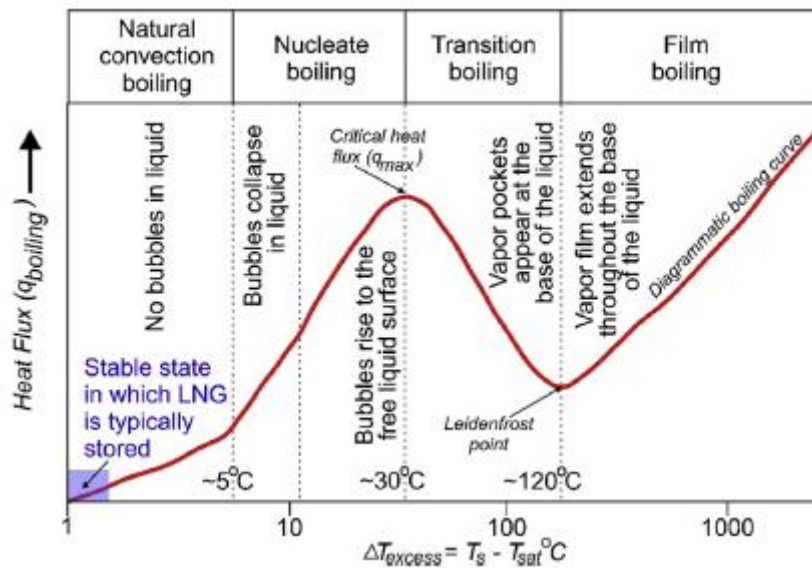


Fig. 2: Boiling curve (Kulitsa and Wood, 2018).

A plot of heat flux,  $q$  against temperature difference between LNG pool and water surface,  $\Delta T_{\text{excess}}$ , is called the boiling curve, sometimes called the Nukiyama curve after the person who first characterized it back in the 1930s (Aursand, 2018). Fig. 2 is an illustration of such a boiling curve of LNG on confined, shallow water. The heat flux between a heat source and a boiling liquid

strongly depends on the temperature difference,  $\Delta T$ . In the case of LNG boiling on confined water, there is large temperature difference otherwise known as superheat, in the beginning of LNG pool formation on water surface. Film boiling regime is marked by formation of vapour film between LNG pool and water surface, and continuous decrease in heat flux. The formed vapour film prevents LNG pool from

being in intimate contact with water surface, which leads to less vapour generation since heat transfer to LNG pool has been reduced. Temperature difference drops gradually, as a result of cooling of water surface by cryogenic LNG and eventual heat loss by water surface. At a point, the heat flux goes through a minimum ( $q_{\min}$ ) which corresponds to onset of formation of vapour pockets. The superheat temperature (excess temperature) at which this happens is termed minimum point temperature,  $\Delta T_{\min}$ , and for saturated liquid like LNG, it is equal to the liquid leidenfrost temperature,  $T_L$ .

Minimum point temperature marks beginning of transition boiling regime during which vapour pockets allow partial contact between LNG pool and water surface underneath, and there is partial collapse and regeneration of vapour film in transition boiling regime. Due to improved contact between LNG pool and water surface, heat flux increases monotonically. This is expected to continue until a critical or maximum heat flux,  $q_{\max}$ , is attained. Superheat temperature at maximum heat flux is termed critical temperature,  $\Delta T_{\text{cri}}$ . Critical heat flux is maximum heat flux for transition boiling regime, beyond critical heat flux, heat flux from water surface to LNG pool wanes down, and this marks onset of nucleate boiling regime. During nucleate boiling regime, vapour film has completely collapsed, and there is intimate contact between LNG pool and underlying water surface, leading to further decrease in superheat temperature due to cooling of water surface by cryogenic LNG pool. As stated earlier, superheat temperature (temperature difference) is the driving force for heat transfer from water surface to LNG pool. Therefore, decrease in superheat temperature encourages decrease in heat flux. Boiling temperature or saturation temperature of a pure liquid substance like methane depends on the applied pressure. In practice, larger volume of LNG vaporises during film boiling. When temperature of water surface drops very close to LNG temperature (stable state in which LNG is stored), transfer of heat from the water surface to the LNG pool is by natural convection as shown in Fig. 2, and hence the heat flux curve decreases slowly.

Vapour from LNG as it returns to a gaseous phase, can cool ambient air molecules to form white dense fume termed vapour cloud, above LNG pool. The formed vapour cloud warms up afterwards, and disperses from the source. If not properly and safely managed can become flammable when concentrated within flammability range, but explosive only under certain well-known conditions, for instance, when it is confined. LNG pool fire may happen if the

vapour cloud above LNG is ignited, but fire seen in dispersing LNG vapour is termed Vapour fire (Ezeh and Okafor, 2022).

For adequate risk assessment and consequence analysis of possible LNG spill on water surface, it is pertinent to develop means of predicting vaporization of LNG pool. Modelling vaporization of LNG pool is key element in risk assessment and consequence analysis of a possible LNG spill on water surface (Wodek, 2019; Yi, 2012). LNG pool spreading, LNG vaporization and LNG vapour dispersion are important physical processes associated with LNG spillage. Difficulty encountered in modelling vaporization of LNG is incorporation of all the aforementioned physical processes, associated with LNG spillage. LNG vaporization models in vogue do not account for effect of LNG pool height on vaporization flux/rate of LNG spilled on water. However, experiments revealed that LNG pool height affects vaporization rate of LNG on confined water surface (Timothy and Harri, 2010). Sequel to the foregoing expose, LNG vaporization model that accounts for effect of LNG pool height on vaporization rate of LNG is proposed.

## 2. Materials and methods

In order to investigate influence of LNG pool height on vaporization of LNG pool, model applicable to LNG spill on confined water surfaces is presented by modifying Vesovic (2006) model, and LNG modelled as pure methane.

$$dM / dt = -m'' R^2 \quad (1)$$

where  $dM$  is the change in mass of liquefied natural gas in kg;  $dt$  is change in time in seconds;  $R$  is liquefied natural gas (LNG) pool radius, in m; while  $m''$  is proportional to vaporization rate per unit area. The modification to derive Equation (2) was done by assuming instantaneous discharge of LNG on water surface in cylindrical enclosure. The enclosure is so small that cryogenic LNG immediately covers the entire area upon spill. Radius of LNG pool is constant once pool spreads to wall of enclosure. It is crucial to consider that mass of LNG spilled is function of density and volume, and LNG pool takes shape of the cylindrical enclosure. Water surface upon which LNG pool buoys can be treated as flat surface throughout the process, and film boiling regime was assumed.

$$-dH / dt = q_x / \rho_{LNG} L_{LNG} \quad (2)$$

where  $dH$ , is change in height of liquefied natural gas (LNG) pool in m;  $dt$  is change in time in seconds;  $q_x$  is heat flux in  $\text{kJ}/\text{sec}\cdot\text{m}^2$ ;  $\rho_{\text{LNG}}$  is density of LNG in  $\text{kg}/\text{m}^3$ ;  $L_{\text{LNG}}$  is latent heat of vaporization of LNG in  $\text{kJ}/\text{kg}$ .

The boiling regime assumed is accounted for by employing suitable heat and heat transfer coefficient equations. Model that will account for vaporization of LNG and LNG pool height increase during LNG spill on confined water surface is proposed, and it is given below.

$$dH/H = -q_x dt / \rho_{\text{LNG}} L_{\text{LNG}} \quad (3)$$

The variables still retain their original definitions;  $H$  is height of LNG pool. Film boiling regime was assumed while driving vaporization Equation (3). Equation (3) was developed on basis of principles of exponential growth equation.

In order to predict vaporization flux/rate of LNG, it is essential to model heat conducted to the LNG pool from water underneath. Conduction is the major mode of heat transfer to LNG pool from the water surface on which the LNG is spilled. Heat gain by LNG pool from other sources is not up to 5% (Webber, 1990; Cook and Woodward, 1993; Cavanaugh et al., 1994). Thus, heat transfer is modelled to be happening only from water on which LNG is spilled. LNG is stored at its boiling temperature. This implies that whole heat gained by the LNG pool is utilized for LNG vaporization. The heat flux to LNG pool across the water-LNG interface during film boiling regime can be expressed with Equation (4):

$$q_x = h(T_w - T_L) \equiv h\Delta T \quad (4)$$

$T_L$  and  $T_w$  are the temperatures of LNG and water respectively,  $h$  is the heat transfer coefficient of LNG. The temperature difference,  $\Delta T$  referred to as the superheat temperature is driving force for heat transfer. Heat transfer coefficient,  $h$ , in Equation (4) does not only depend on thermo-physical properties of the participating fluids, but also depends on type of boiling regime that occurs. In this research work, correlation developed by Klimenko (1980) for boiling of saturated liquids on horizontal plate has been used. The film boiling heat transfer coefficient,  $h_f$ , is giving by

$$h_f = \lambda_v N_u / l_c \quad (5)$$

$\lambda_v$  is thermal conductivity of LNG vapour, its value is  $1.24 \times 10^{-4} \text{ W}/\text{m}\cdot\text{K}$ .  $N_u$  is Nusselt number;  $l_c$  is critical wavelength of Taylor instability which is given by the Equation (8).

$$l_c = 2\pi[\sigma / g(\rho_l - \rho_v)]^{1/2} \quad (6)$$

$\sigma$  is surface tension of the liquid-vapour interface, its value is  $0.014 \text{ N}/\text{m}$ ;  $\rho_l$  is density of LNG,  $\rho_l = 423 \text{ kg}/\text{m}^3$ ;  $\rho_v$  density of LNG vapour film,  $\rho_v = 0.657 \text{ kg}/\text{m}^3$ . Nusselt number,  $N_u$  in Equation (5) is given by Equation (7) for laminar vapour flow through layers of vapour film.

$$N_u = 0.19[A_r P_r]^{1/3} f_1 \quad (7)$$

$A_r$  is Archimedes number;  $P_r$  is Prandtl number of vapour phase;  $f_1$  is near unity correction factor whose values depend on superheat temperature as shown in Equations (8) and (9).

$$f_1 = 1 \quad \text{at} \quad r / C_p \Delta T \leq 1.4 \quad (8)$$

$$f_1 = 0.89(r / C_p \Delta T) \quad \text{at} \quad r / C_p \Delta T > 1.4 \quad (9)$$

Archimedes number is defined by expression (10) such that vapour flow via layers of vapour film is laminar when  $A_r < 10^8$ .

$$A_r = (2\pi)^3 \sigma^{3/2} \rho_v V_v^2 \sqrt{g(\rho_l - \rho_v)} \quad (10)$$

$V_v$  is the viscosity of the vapour phase,  $V_v = 6.287 \times 10^{-3} \text{ N}\cdot\text{s}/\text{m}^2$ . Prandtl number,  $P_r$  is given by

$$P_r = \mu_v C_p / \lambda_v \quad (11)$$

$\mu_v$  is the viscosity of the vapour phase,  $\mu_v = 6.287 \times 10^{-3} \text{ N}\cdot\text{s}/\text{m}^2$ ;  $C_p$  is specific heat capacity of LNG vapour,  $C_p = 2.087 \text{ KJ}/\text{kg}\cdot\text{K}$  at  $200 \text{ K}$ .

The temperature of the surface of water in contact with LNG is determined by the quantity of heat conducted to the water surface. Heat conduction through water body can be represented by the Fourier's heat equation; it is presumed that the dominant mode of heat transfer direction is vertical upwards,  $y$ -direction in Equation 12, thus making the water temperature distribution one-dimensional (1-D), provided that thermal boundary layer in water is small.

$$dT_w / dt = K_w (d^2 T_w / dy^2) \quad (12)$$

where  $K_w$  is the thermal diffusivity of water, with numerical value of  $1.4558 \times 10^{-7} \text{ m}^2/\text{s}$ . The variation of the water surface temperature with time is then given by,

$$T_w = T_b + (T_o - T_b) \exp(-t^*) \operatorname{erfc}(\sqrt{t^*}) \quad (13)$$

$$\text{Reduced time, } t^* = (h^2 / \lambda_w^2) k_w t \quad (14)$$



$T_0$  is initial temperature of water surface;  $T_w$  is the temperature of water surface at time,  $t$ , while  $T_b$  is LNG boiling temperature,  $\lambda_w$  is thermal conductivity of water,  $\lambda_w$  is equal to 0.598 W/m. K.

A purely analytical approach was used to solve the present model, and solution was implemented in FORTRAN environment, an integrated development environment. A number of simulations were run to study changes in variables of interest, using 288 K as initial temperature of water surface. LNG was assumed to be released at its boiling point (112 K). Program written in FORTRAN language for film boiling, simulates the behaviour of liquefied natural gas (LNG) and water over a given time period. It calculates the changes in water temperature, LNG height, and vaporization flux/rate at each time step.

### 3. Results and discussion

Fig. 3 is profile of temperature of water surface against time. Fig. 3 shows temperature of water surface at each time step, during film boiling regime following LNG spill. For the first 5 seconds, drop in temperature of water surface was steep, but, it slowed down afterwards because of decrease in temperature difference between LNG and water surface. Results obtained show that temperature of water surface decreased to fixed value of 112.8877 K, a value close to LNG boiling point. Temperature of water surface dropped due to cooling by cryogenic LNG released on it. The results show strong agreement with Vesovic's result. According to analysis, to maintain the surface temperature of water within 10 degrees Celsius of its original temperature during spills lasting up to 5 minutes, the effective thermal conductivity needs to be about three orders of magnitude greater than the molecular thermal conductivity. Vesovic's model, designed for exploratory or educational purposes, substituted the molecular thermal conductivity with an effective parameter. However, in the current model aiming to simulate real-life LNG spills on water surfaces, Vesovic's recommendation was disregarded.

Fig. 4 is profile of heat transfer coefficient against time. Fig. 4 is heat transfer coefficient-time profile obtained by implementing model solution in FORTRAN environment. It shows at a glance, heat transfer coefficient of LNG at each time step during film boiling regime. As expected, temperature difference-dependent heat transfer coefficient decreased rapidly, from peak value of 645.5825 W/m<sup>2</sup> at the beginning of the LNG pool lifetime, but, it can be seen in Fig. 4, that the heat transfer coefficient later decreased gradually to fixed value

of 6.4782 W/m<sup>2</sup>. The heat transfer coefficient depends on temperature difference between water surface and cryogenic LNG, thus, heat transfer coefficient varies directly with temperature difference. Higher temperature difference necessitates higher heat transfer coefficient, cryogenic LNG gaining more heat sufficient for vaporization. The heat transfer coefficient also depends on the boiling regime that occurs. At onset of film boiling, there is intimate contact between water surface and LNG which facilitates heat transfer from water surface to LNG. However, LNG vapour generated forms thin film between water surface and LNG preventing intimate contact, this limits heat transfer from water to LNG at later part of film boiling. Moreover, heat transfer coefficient varies inversely with surface tension. At later part of film boiling, the tension of surface film tends to minimize surface area of contact, thereby, decreasing heat transfer coefficient.

Fig. 5 is profile of heat flux against water-LNG temperature difference. Curve in Fig. 5 shows variation of heat flux with water-LNG temperature difference during film boiling regime. The heat flux between a heat source and a boiling liquid strongly depends on the temperature difference,  $\Delta T$ . In the case of LNG boiling on confined water, there is large temperature difference (6.5434 K) otherwise known as superheat, in the beginning of LNG pool formation on water surface, hence, large heat flux (312.446 KJ/m<sup>2</sup>.s) from water surface to LNG pool. Temperature difference drops gradually, as a result of cooling of water surface by cryogenic LNG and eventual heat loss by water surface. At a point, the heat flux goes through a minimum ( $q_{min}$ ) value of 6.3665 KJ/m<sup>2</sup>.s which corresponds to onset of formation of vapour pockets.

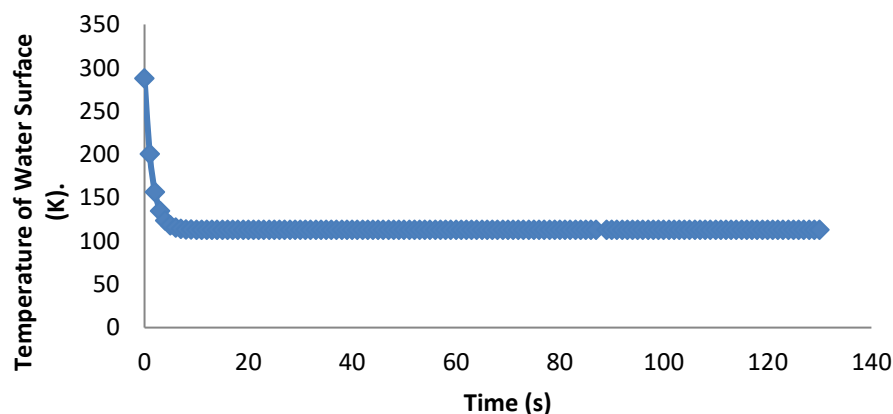
Fig. 6 is profile of heat flux against time. The results were obtained by running simulations in FORTRAN environment. Fig. 6 shows heat flux from underlying water to LNG pool during film boiling. The heat flux was seen to be maximum in the beginning of LNG boiling (film boiling), The maximum outputted heat flux was 297.6808 KJ/m<sup>2</sup>.s after 5 seconds, at this time, heat transfer driving force was still high. Heat flux from water to LNG pool decreased rapid in the beginning of LNG boiling, this was caused by vapour produced, which then formed film between LNG pool and water surface (heat source), preventing intimate contact between the fluids. After initial sharp drop in heat flux, heat flux decrease was seen to happen gradually for some seconds as it approaches a minimum value. After 28 seconds, heat flux was seen to have dropped to minimum value of 5.7509

$\text{KJ/m}^2\cdot\text{s}$  for film boiling. Though, the study was limited to film boiling, LNG boiling mode was expected to change if heat flux drops below the minimum,  $q_{\min}$ .

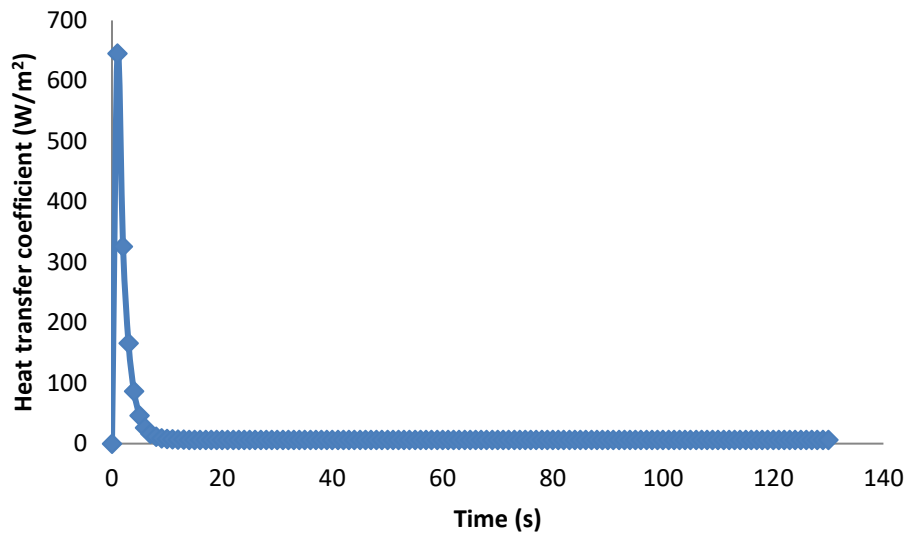
Fig. 7 is profile of LNG vaporization flux against time while Fig. 8 is profile of LNG vaporization against time. Fig. 7 and Fig. 8, obtained by implementing solution of present model in an integrated development environment, show vaporization flux and vaporization rate respectively, at each time step following LNG spill on confined water surface. Vaporization flux and vaporization rate increased monotonically and attained maximum values of  $3.0456 \text{ kg/m}^2\cdot\text{s}$  and  $0.3828 \text{ kg/s}$  respectively, after 2 seconds. Increase in vaporisation flux/rate during LNG release can be attributed to large heat flux from underlying water surface to LNG pool in the beginning of the film boiling mode, which is driven by large temperature difference between water surface and LNG pool. These results agree favourably with Horvat (2019) in the sense that vaporization flux/rate and heat flux are maximum at the initial point of LNG release, when direct contact between LNG and water surface still exists. The fluxes decrease gradually afterwards due to formation of protective vapour film between water surface and LNG pool, which reduces heat flux from water surface to LNG. Hence, eventual decrease in vaporisation flux/rate.

Fig. 9 is profile of LNG pool height against time. The results were obtained by performing simulations in FORTRAN environment. Fig. 9 shows height of LNG pool in the confinement at each time step. It is evident in Fig. 9 that LNG pool height reached peak value of 7.2 m, same time (2 seconds) vaporization flux and vaporization rate attained maximum values. Due to scarcity of experimental data on this subject, it is ethical to be prudent at this stage. Nevertheless, Timothy and

Harri's experimental data shows dependence of LNG vaporization rate on LNG pool height spilled on confined water surface. The correlation amongst LNG vaporization flux/rate and height of LNG on confined water surface can be attributed to the fact that boiling or saturation temperature of a pure liquid substance like methane depends on pressure (Bijoy et al., 2022). Mass transfer type of equation that relates boiling rate, pseudo mass transfer coefficient and pressure differential can be easily employed to explain influence of liquefied natural gas pool height on vaporization flux/rate. Boiling of liquid starts when its saturated vapour pressure becomes equal to or greater than external pressure on the liquid, or greater than the pressure in the vapour phase above the liquid. As long as the liquid and vapour are not in equilibrium, the driving force of the boiling rate is the pressure differential. Pressure is usually low at elevated heights such that liquid boils faster. Depressions conveniently lowers pressure differential so that liquid boils slower. Besides, along vapour saturation line on P-V diagram, pressure decreases with increase in volume. Volume of LNG on confined water surface is directly proportional to height of LNG pool, provided that LNG pool radius is constant. Vaporization is bulk phenomenon, and boiling happens in whole parts of the given liquid. Since total kinetic energy of the system can be equated to total potential energy, effusion speed of LNG vapour can be found to be directly proportional to LNG pool height in the enclosure. From all indications, results of present model agree favourably with Timothy and Harri's experimental data. Lower LNG pool heights consistently yielded lower vaporization rates/fluxes, and vaporization rate/flux decreased gradually after attaining maximum value.



**Fig. 3:** Temperature of water surface – time profile at initial temperature of 288 K.



**Fig. 4:** Heat transfer coefficient-time profile at initial temperature of 288 K.

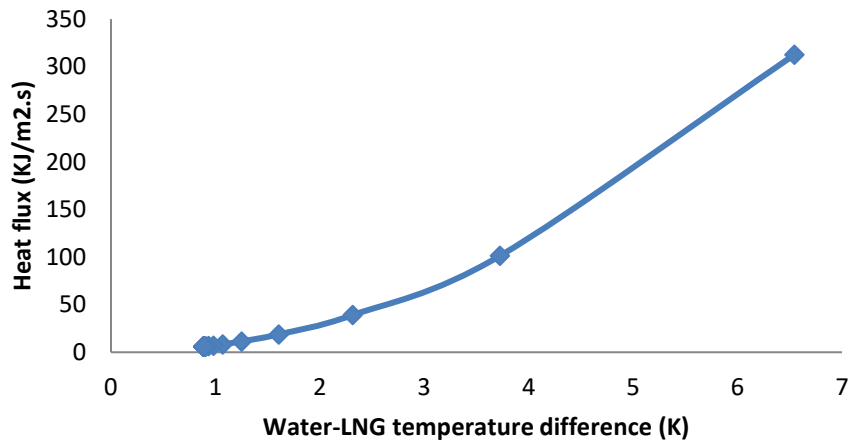


**Fig. 5:** Profile of heat flux against water-LNG temperature difference during LNG film boiling.

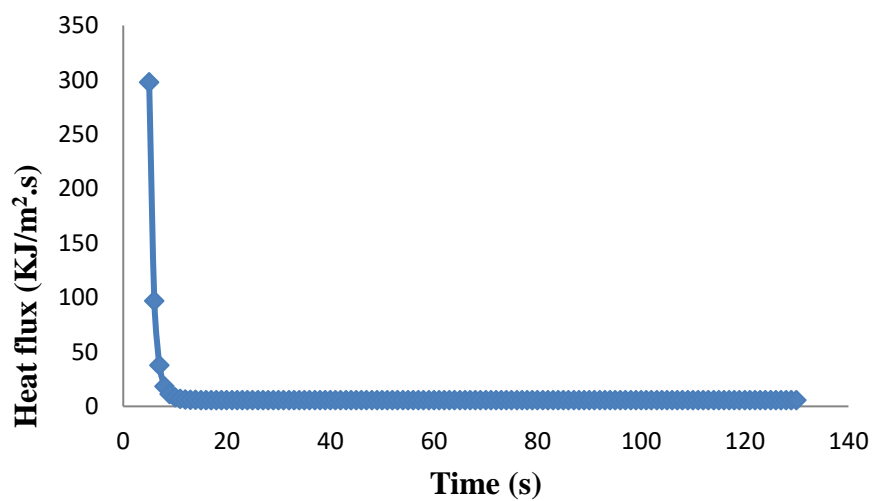


**Fig. 6:** Heat flux-time profile at initial temperature of 288 K.

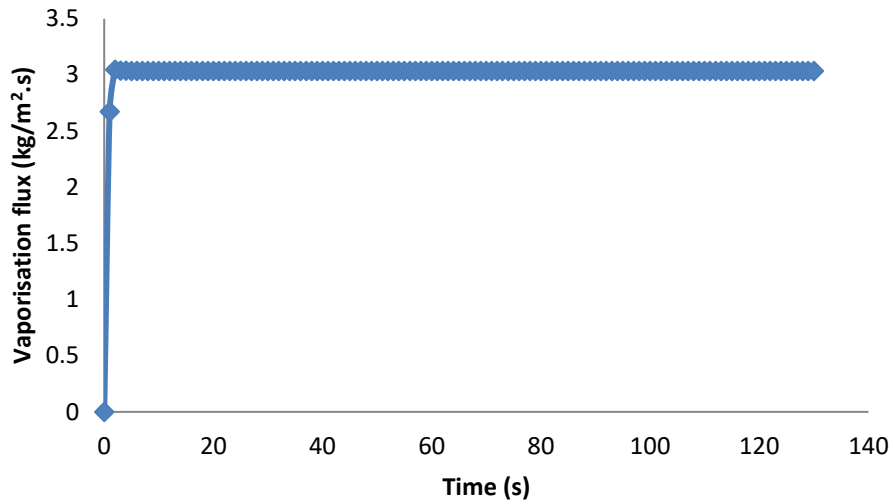


Fig. 7: LNG vaporization flux-time profile at initial temperature of 288 K.

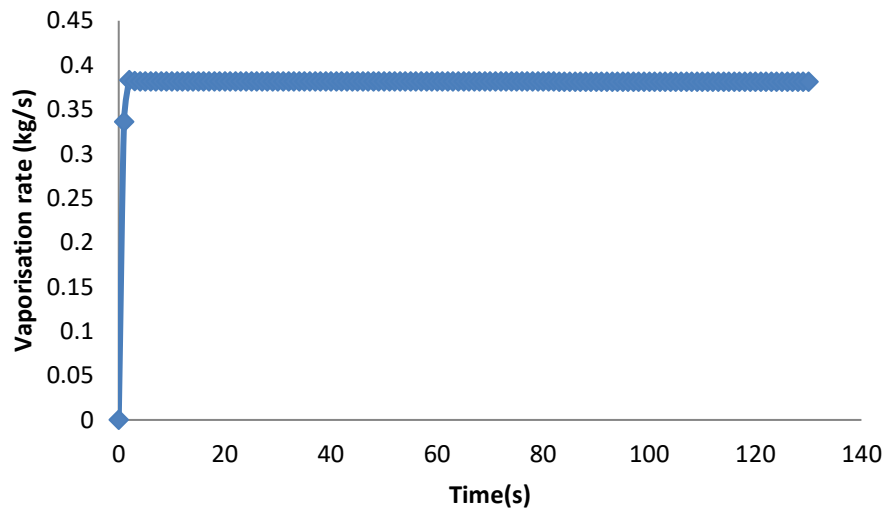


Fig. 8: LNG vaporization rate-time profile at initial temperature of 288 K.

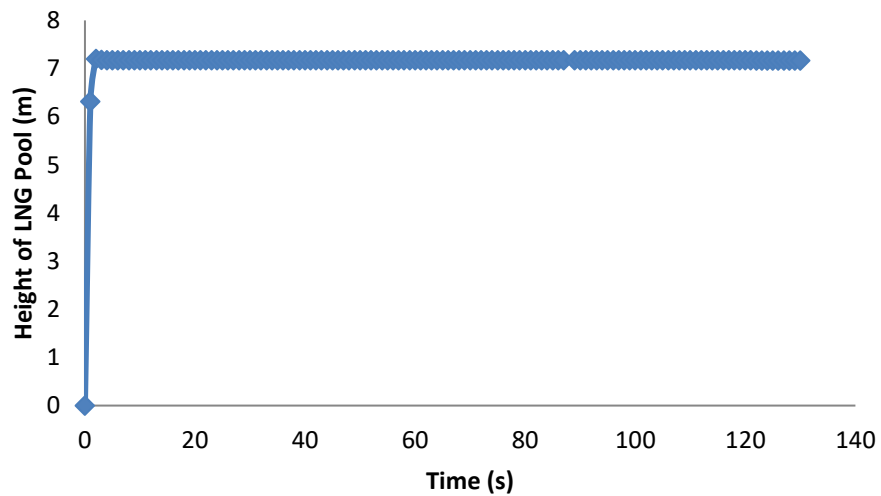


Fig. 9: LNG pool height-time profile during film boiling at initial temperature of 288 K.



#### 4. Conclusion

LNG spill on confined water surface cools water surface, causing temperature drop. During film boiling regime of LNG pool on confined water surface, heat flux from underlying water surface to LNG pool decreases alongside water surface temperature. Rate of vaporization of LNG pool on confined water surface depends on temperature of water surface, amount of heat conducted to the pool, LNG pool boiling mode amongst other factors. It has been shown by means of present model that vaporization of LNG pool on confined water surface is influenced by height of the LNG pool, since vaporization flux/rate attains crest and trough same time as LNG pool height, provided that LNG pool radius is constant.

#### References

- Aursand, E. and Morten, H. (2018) Predicting triggering and consequence of delayed LNG RPT. Article in *Journal of Loss Prevention in the Process Industries*, 55: 124–133
- Bijoy, K.P., Zakir, H. and Prasad, P.S. (2022) *Boiling and Condensation in: Heat Transfer Fundamental, Enhancement and Applications*, IntechOpen, London, United Kingdom, 1st Edition: 3-24.
- Cavanaugh, T.A., Siegel, J.H. and Steinberg, K.W. (1994) Simulation of vapour emissions from the liquid spills, *Journal of Hazardous Materials*, 38, 41-63.
- Cook J. and Woodward J.L. (1993) A new integrated model for pool spreading, evaporation and solution on land and water, *International Conference on Health, safety and loss prevention in the oil, chemical and process industry*, Butterworth, Oxford, pp 359-370.
- Ezeh, E.A. and Okafor, E. (2022) A Review of LNG Vaporization Rate Models for Water Spills. *International Journal of Innovative Science, Engineering and Technology*, 9(11): 2348-7968.
- Klimenko, V.V. (1980) Film boiling on a horizontal plate - new correlation. *International Journal of Heat and Mass Transfer*, 24(1):69–79.
- Kulista, M. and Wood, D.A. (2018) Floating storage and regasification units face specific LNG rollover challenges: Consideration of saturated vapour pressure provides insight and mitigation options, *Natural Gas Industry B*, 5(4): 391-414.
- Michelle, M.F., Volkov, D. and Analyst, E. (2012) LNG Safety and Security, Centre for Energy Economics, Bureau of Economic Geology, Jackson School of Geosciences, The University of Texas at Austin, 2(1).
- Timothy, L.M and Harri, K.K. (2010) The Effect of Turbulence on Rate of Evaporation of Cryogenic LNG and LN<sub>2</sub> on Water. 13th Annual Symposium, Mary Kay O'Connor Process Safety Center "Beyond Regulatory Compliance: Making Safety Second Nature" Texas A&M University, College Station, Texas.
- Vesovic, V. (2006) The Influence of Ice Formation on Vaporization of LNG on Water Surfaces. *Journal of Hazardous Material*, 140: 518-526.
- Webber, D.M. (1990) Model for pool spreading and vaporization and its implementation in computer code GASP, UKAEA Report SRD R 507.
- Wodek, T. (2019) Analysis of Boil-off Rate Problem in Liquefied Natural Gas Receiving Terminals. 2nd International Conference on the Sustainable Energy and Environmental Development, IOP Conference Series, Earth and Environmental Science 214, 012105.
- Yi, L., Xiaodan, G., Tomasz, O., Luc, V. and Sam, M.M. (2012) Modelling the Vaporization of Cryogenic Liquid Spilled on the Ground Considering Different Boiling Phenomena, *Institute of Chemical Engineers, Symposium Series No. 158*.